BASIC SCIENCE

Nanomedicine: Nanotechnology, Biology, and Medicine 6 (2010) 689–697

nanomedicine

www.nanomedjournal.com

Original Article

Discriminated effects of thiolated chitosan-coated pMMA paclitaxel-loaded nanoparticles on different normal and cancer cell lines

Seyedeh Parinaz Akhlaghi, PharmD[a], Shahrooz Saremi, PharmD[a], Seyed Nasser Ostad, PhD[a], Rassoul Dinarvand, PhD[a,b], Fatemeh Atyabi, PhD[a,b,*]

[a]*Faculty of Pharmacy, Tehran University of Medical Sciences, Tehran, Iran*

[b]*Medical nanotechnology Research Centre, Medical Sciences/University of Tehran, Tehran, Iran*

Received 14 September 2009; accepted 25 January 2010

Abstract

The aim of the present work was to prepare and characterize poly(methyl methacrylate) nanoparticles coated by chitosan–glutathione conjugate so as to encapsulate insoluble anticancer drugs. Nanoparticles were synthesized through radical polymerization of methyl methacrylate initiated by cerium (IV) ammonium nitrate. Paclitaxel (PTX), a model anticancer drug, was encapsulated in nanoparticles with a maximal encapsulation efficiency of 98.27%. These nanoparticles showed sustained in vitro release of the incorporated PTX (75% of the loaded dose was released in 10 days). All nanoparticles had positive charge and were spherical, with a size range of about 130–250 nm. The PTX-loaded nanoparticles showed cytotoxicity for NIH 3T3 and T47D breast carcinoma cells, along with no cytotoxicity for two colon cell lines (HT29, Caco2).

From the Clinical Editor: The aim of this work was to prepare and characterize poly(methyl methacrylate) nanoparticles coated by chitosan–glutathione conjugate in an effort to encapsulate Paclitaxel as a model of insoluble anticancer drugs. These nanoparticles showed sustained in vitro drug release.

Key words: Thiolated chitosan; Nanoparticles; Poly(methyl methacrylate); Paclitaxel; Cytotoxicity

Paclitaxel (PTX), a major anticancer drug isolated from the bark of the Pacific yew tree (*Taxus brevifolia*), has antineoplastic activity against various types of solid tumors including breast cancer, advanced ovarian carcinoma, lung cancer, head and neck carcinomas, and acute leukemias.[1,2] The mechanism of action of PTX is unique. It disrupts the dynamic equilibrium within the microtubule system and blocks cells in the late G2 and M phases of the cell cycle, thus inhibiting cell replication.[3] PTX is poorly soluble in water and many other pharmaceutically acceptable solvents. To enhance its solubility and allow parenteral administration, PTX, currently formulated as Taxol (Bristol-Myers Squibb, Sermoneta, Italy), is dissolved in a 50:50 (vol/vol) mixture of the surfactant Cremophor EL (polyoxyethylated castor oil;) and dehydrated ethanol. Cremophor EL (BASF, Ludwigshafen, Germany) causes acute hypersensitivity reactions in 2% to 4% of patients.[4,5] It can also cause neurotoxicity, nephrotoxicity, and effects on endothelium and vascular muscles, leading to vasodilatation, labored breathing, lethargy, and hypotension.[6]

Researchers are attempting to formulate PTX in a delivery system without the use of Cremophor EL for better solubility. These systems include micelles, nanoparticles, liposomes, co-solvent systems, emulsions, and various conjugates[7] Among these delivery systems being applied to PTX, nanoparticles are considered to be effective carriers. Incorporation of anticancer drugs into the nanoparticles, due to changes in the pharmacokinetics or tissue distribution, reduces the adverse reactions and increases the therapeutic efficacy.[8]

Chitosan (Cht) and its derivatives are useful polymeric biomaterials in the biomedical area and are widely used polysaccharides for different pharmaceutical purposes.[9] Cht is biocompatible, biodegradable, and nontoxic, and shows mucoadhesion properties by establishment of electrostatic interactions with sialic groups of mucin.[10] Chitosan includes various chemical groups that can be grafted by different ligands at the surface of the particles. This results in systems with high specificity. One chemical modification of Cht involves grafting thiol groups in the polymer structure.[11,12] Thiolated chitosans

*Corresponding author: Faculty of Pharmacy, Tehran University of Medical Sciences, Tehran, PO Box 14155-6451, Iran.

E-mail address: atyabifa@tums.ac.ir (F. Atyabi).

1549-9634/$ – see front matter © 2010 Published by Elsevier Inc.
doi:10.1016/j.nano.2010.01.011

improve mucoadhesive properties by forming disulfide bonds with the cysteine-rich domains of mucus glycoproteins.[13] Also, thiolated chitosans develop additional mucosal permeation-enhancing properties by a glutathione-regeneration mechanism.[14,15] To make use of these novel multifunctional polymers for poorly absorbed drugs, such as PTX, in this study an appropriate core shell nanoparticle delivery system, based on utilizing advantage of a polysaccharide, is prepared. This system contains a derivative of Cht, a hydrophilic polymer, in the shell and a hydrophobic drug in the core.

We chose PTX as a model anticancer drug because of its excellent therapeutic effects against a wide spectrum of cancers. Nanoparticle surface modifications were made by application of thiolated Cht with different molecular weights in the particle shell.

The PTX-loaded chitosan–L-glutathione reduced form (Cht-GSH)–coated poly(methyl methacrylate (pMMA) nanoparticles were prepared by a radical polymerization method and were then characterized by laser light scattering for particle size and size distribution. Laser Doppler electrophoresis was used to determine surface charge, and scanning electron microscopy (SEM) and transmission electron microscopy (TEM) were used for studying surface morphology. The physical status of PTX in the nanoparticles was characterized by differential scanning calorimetry (DSC). Drug encapsulation efficiency and drug loading in the nanoparticles and the in vitro drug release profile were measured by high-performance liquid chromatography. The mucoadhesion properties of the nanoparticles were determined by mucus glycoprotein assay. In the present study, to permit observation of various potential mechanisms of cytotoxicity of formulated products, we examined the cytotoxicity of PTX-loaded nanoparticles on two human colon carcinoma cell lines, as well as one breast carcinoma cell line and one nonhuman normal fibroblast cell line. This study might lead to a carrier system for improving the efficacy of water-insoluble anticancer drugs.

To the best of our knowledge, this is the first time PTX, a model for insoluble anticancer drugs, has been encapsulated in thiolated Cht-coated pMMA nanoparticles. These nanoparticles were chosen to take advantage of a core-shell nanoparticle delivery system that is based on thiolated Cht, a hydrophilic, biocompatible, and mucoadhesive polymer, in its shell and incorporating a hydrophobic drug in the core.

Methods

Materials

PTX was supplied from Cipla (Mumbai, India); Cht, with a medium molecular weight and degree of deacetylation of about 89%, was supplied from Primex (Karmoy, Norway). GSH, 1-ethyl-3-(3-dimethyl amino-propyl) carbodiimide hydrochloride (EDAC), *N*-hydroxysuccinimide, methyl methacrylate (MMA), cerium (IV) ammonium nitrate, sodium nitrite ($NaNO_2$), hydrochloric acid (HCl), glacial acetic acid, sodium hydroxide (NaOH), mucin, basic fuchsin, periodic acid, sodium metabisulfite, ethyl cellulose, Carbomer 940, Tween 80, and potassium hydrogen phosphate were all purchased from Merck (Darmstadt, Germany). All chemicals were of analytical grade. 3-(4,5-dimethylthiazol-2-yl)-2,5-diphenyl tetrazolium bromide) (MTT) was purchased from Sigma-Aldrich (St. Louis, Missouri). Cell lines were obtained from Pasteur Institute (Tehran, Iran)

Chitosan depolymerization

Cht was depolymerized by a chemical reaction so as to obtain the desired low, medium, and high molecular weights of Cht as follows. Ten milliliters of solutions of $NaNO_2$ in deionized water at different concentrations (7.0, 2.7, and 1.6 g/L) were added to the solution of Cht (2 g of medium-molecular-weight Cht in 100 mL of acetic acid 6% vol/vol) at room temperature (15-25°C) under stirring for 1 hour. Reduced-molecular-weight Cht forms were precipitated by adding a solution of NaOH (4 M) reaching pH 9.0. The white-yellowish precipitate was filtered, washed three times with acetone, and redissolved in a minimum volume of acetic acid (0.1 M). Purification was carried out by subsequent dialyses (Sigma dialyses tubes MW cutoff 12 kDa) against 1 L deionized water (twice for 90 minutes and once overnight). The dialyzed product was freeze-dried (LyoTrap plus; LTE Scientific, Oldham, United Kingdom) and then stored at 4°C. Products obtained were called: Cht_{low}, Cht_{med}, and Cht_{high} based on their theoretical molecular weight.

Measurement of molecular weight

The molecular weights of hydrolyzed chitosans were determined by gel permeation chromatography (GPC) using pullulane (Showa Denko, Kawasaki, Japan) standards. A PL Aquagel-OH mixed gel filtration column (300 mm × 7.5 mm internal diameter, pore size 8 μm) from Agilent Technologies (Santa Clara, California) was used. All chromatograms were generated on an Agilent 1100 Liquid Chromatographer (Agilent Technologies), and the eluting fraction was monitored using a refractive index signal detector. The mobile phase consisted of 0.2 M acetic acid and 0.1 M sodium acetate at a flow rate of 4 mL/min. The chromatographic procedures were carried out at 23°C. Thirty milligrams of depolymerized chitosans were dissolved in 10 mL of 0.2 M acetic acid and 0.1 M sodium acetate. The mixture was analyzed by the GPC system using the narrow method.

Preparation of chitosan-glutathione conjugate

The covalent attachment of GSH to Cht, achieved by formation of amide bonds between amine groups of Cht and carboxylic acid moieties of GSH, was carried out based on a slightly modified method described before[16] as follows: 1.000 g of GSH, 0.912 g EDAC, and 0.552 g *N*-hydroxysuccinimide were added to the solution of Cht dissolved in HCl (0.1 M). The pH was set to 6.0 with 5.0 M NaOH, and kept stirring for 15 hours at room temperature. To omit unbound reagents, the resulting GSH-conjugated Cht (Cht-GSH) was dialyzed in tubing [molecular weight (MW) cutoff 12 kDa], first against 5 mM HCl for 12 hours, twice against 5 mM HCl containing 1% NaCl each for 12 hours, and finally two times against 1 mM HCl each for 12 hours. Prepared polymers were lyophilized at –50°C and 0.01 mbar (LyoTrap plus; LTE Scientific) and stored at 4°C for further use.

Table 1
Molecular weights of depolymerized chitosan and thiolated chitosan characterization (n = 3)

Chitosan type	$NaNO_2$ (mg/mL)	Determined MW (g/mol)	Free thiol (μmol/g)	Disulfide bound (μmol/g)	Total amount of sulfhydryl groups (μmol/g)
Cht_{low}	7.0	15,520 ± 1262	92.81 ± 6.79	594.51 ± 44.71	687.32 ± 48.37
Cht_{med}	2.7	32,007 ± 2960	81.67 ± 5.26	521.67 ± 10.50	603.34 ± 13.55
Cht_{high}	1.6	87,116 ± 7543	75.77 ± 5.82	491.31 ± 35.03	567.08 ± 29.96

MW, molecular weight.

Table 2
Size, zeta potential, and PDI of nanoparticles (n = 3)

Nanoparticle	Size (nm)	Zeta potential (mV)	PDI
Cht_{low}-GSH	148 ± 7	47.3 ± 3.2	0.059 ± 0.008
Cht_{med}-GSH	195 ± 19	54.8 ± 3.8	0.084 ± 0.017
Cht_{high}-GSH	223 ± 27	44.5 ± 1.1	0.184 ± 0.046
Cht_{low}	149 ± 20	39.3 ± 2.9	0.373 ± 0.081
Cht_{med}	187 ± 23	41.2 ± 2.0	0.051 ± 0.007
Cht_{high}	231 ± 31	45.7 ± 4.3	0.198 ± 0.039
Cht_{low}–GSH–1% PTX	196 ± 30	36.3 ± 3.4	0.065 ± 0.017
Cht_{low}–GSH–2% PTX	133 ± 19	33.5 ± 4.1	0.443 ± 0.381
Cht_{low}–GSH–3% PTX	141 ± 28	34.1 ± 6.0	0.069 ± 0.054
Cht_{low}–GSH–4% PTX	144 ± 9	30.1 ± 1.8	0.137 ± 0.020
Cht_{low}–GSH–5% PTX	164 ± 23	37.8 ± 3.6	0.200 ± 0.038
Cht_{med}–GSH–1% PTX	203 ± 18	29.7 ± 1.2	0.046 ± 0.061
Cht_{high}–GSH–1% PTX	235 ± 27	34.3 ± 2.2	0.114 ± 0.120
Cht–GSH–1% PTX	241 ± 33	48.7 ± 5.3	0.411 ± 0.078
Cht–3% PTX	136 ± 12	35.2 ± 2.1	0.057 ± 0.011

GSH, L-Glutathione reduced form; PDI, polydispersity index; PTX, paclitaxel.

Determination of the thiol group content of Cht-GSH

For quantifying the total amount of sulfur fixed on Cht-GSH, in disulfide bonds or its reduced form, iodine titration was performed.[10] Briefly, 20 mg of the lyophilized thiolated polymer were hydrated in 6 mL of demineralized water. After the pH was set to 2–3 with 1 M HCl, the solution became clear. Then 500 μL of aqueous starch solution (1%) were added. The samples were titrated with an aqueous iodine solution (1 mM) until a permanent light-blue color was maintained.

Preparation of blank and paclitaxel-loaded core-shell nanoparticles

Grafts of different depolymerized unmodified chitosans or Cht-GSH onto pMMA, and nanoparticle preparation were carried out by radical polymerization.[17] Cht or Cht-GSH (37.5 mg) was dissolved in 4 mL of nitric acid (0.2 M) in a two-necked flask at 40°C under gentle stirring and nitrogen bubbling. After 10 minutes, 1 mL of a solution of 0.08 M cerium (IV) ammonium nitrate in 0.2 M nitric acid was added. For preparation of blank nanoparticles, 0.25 mL of MMA was added under vigorous magnetic stirring. For the procedure of preparing PTX-loaded nanoparticles with 1%, 2%, 3%, 4%, and 5% (PTX/polymers wt/wt), 2.7 mg, 5.4 mg, 8.1 mg, 10.9 mg, and 13.6 mg PTX were dissolved in 0.5 mL methanol, respectively. Then, 0.25 mL MMA was added to the solution. The resulting solution was added to the two-necked flask at 40°C under vigorous magnetic stirring. Then, for both blank and PTX-loaded nanoparticles, nitrogen bubbling was maintained for another 10 minutes and then continued at 40°C under stirring for 30 minutes. After cooling to room temperature, 1 M NaOH was added to adjust the pH to 4.5.

The nanoparticle suspensions were purified by introducing them into a dialysis tube (dialysis tubes MW cutoff 12 kDa; Sigma) against a 16 μmol/L acetic acid solution in deionized water twice for 90 minutes and once overnight. Dry nanoparticles were obtained by lyophilization and stored at 4°C until further use.

Characterization of drug-loaded nanoparticles

Measurement of particle size

The hydrodynamic mean diameter of all blank and PTX-loaded nanoparticles was determined by dynamic light scattering using Zetasizer (Nano-ZS; Malvern Instruments, Worcestershire, United Kingdom). All measurements were performed with a wavelength of 633 nm at 25°C with an angle detection of 90.0 degrees. The samples were diluted in deionized water (1:5 vol/vol), and three subsequent measurements were determined for each sample.

Determination of zeta potential

The zeta potential of prepared nanoparticles was determined by laser Doppler electrophoresis using Zetasizer (Nano-ZS; Malvern Instruments). The samples were diluted (1:5 vol/vol) in deionized water. Each sample was measured three times.

Scanning electron microscopy

The surface morphology of nanoparticles was observed using a scanning electron microscope (XL 30; Philips, Eindhoven The Netherlands). Nanoparticle suspensions were fixed on an aluminum disk and dried at room temperature. The dried nanoparticles were coated with gold metal using a sputter coater (SCD 005; Bal-Tec, Balzers, Switzerland).

Transmission electron microscopy

A transmission electron microscope (CEM 902A; Zeiss, Oberkochen, Germany) was used to observe the two-dimensional, relative size morphology of PTX-loaded nanoparticles. Nanoparticle suspensions were diluted in deionized water (1:100 vol/vol), and before observation nanoparticles were negatively stained with a solution of 1% phosphotungstic acid.

Drug analysis

Drug analysis was carried out applying a high-performance liquid chromatography method as follows: A reverse phase C_{18} column (25 × 0.46 cm internal diameter, pore size 5 μm; Teknokroma, Barcelona, Spain) was used as the stationary

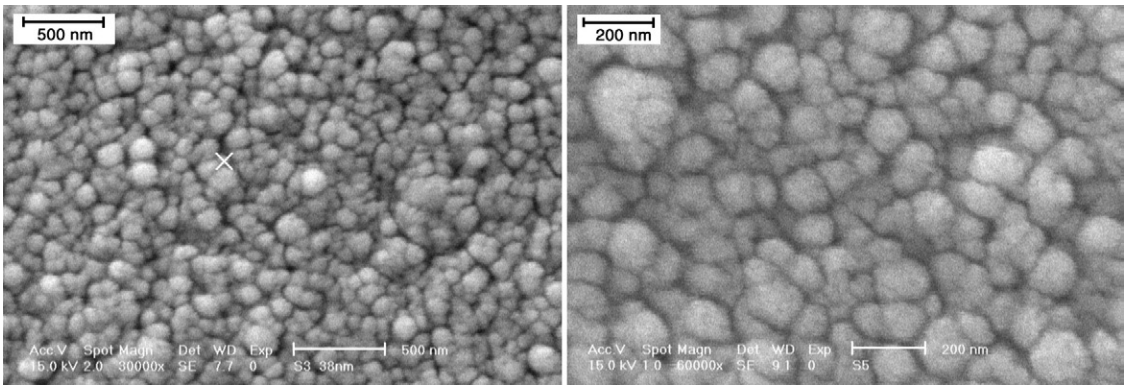

Figure 1. Scanning electron micrographs of paclitaxel-loaded nanoparticles.

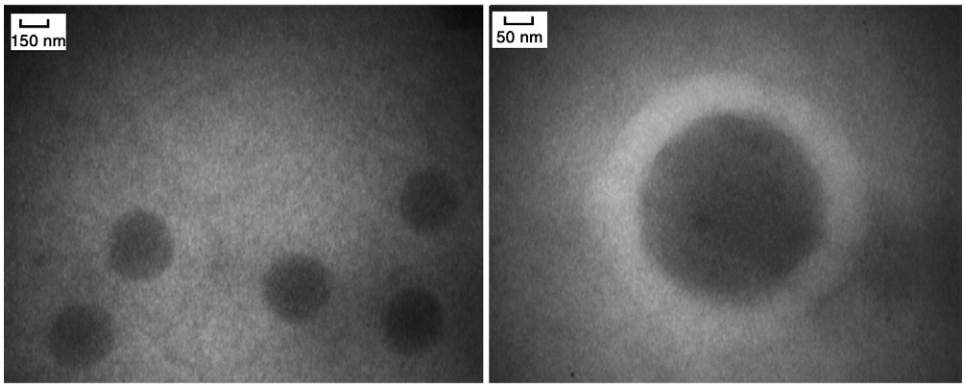

Figure 2. Transmission electron micrographs of paclitaxel-loaded nanoparticles.

phase. The mobile phase consisted of acetonitrile in water (60:40 vol/vol). Separation was carried out at a flow rate of 1 mL/min with a pump (WellChrom, K-1001; Knauer, Berlin, Germany). The run time was 10 minutes for each sample. PTX was detected at a wavelength of 227 nm.

Encapsulation efficiency of nanoparticles and loading efficiency were determined indirectly through measurement of the free drug remaining unloaded in the reaction medium, applying the following equations:

$$\textit{Encapsulation Efficiency}\ (\%) = \frac{\textit{Weight of drug found loaded}}{\textit{Weight of drug unput}} \times 100$$

$$\textit{Drug Loading}\ (\%) = \frac{\textit{Weight of drug found loaded}}{\textit{Weight of nanoparticle}} \times 100$$

Physical status of PTX in the nanoparticles

The physical status of PTX inside the PTX-loaded nanoparticles was determined by DSC (DSC 822^e; Mettler Toledo, Greifensee, Switzerland). The samples were purified with dry nitrogen at a flow rate of 10 mL/min. The temperature was increased at a rate of 10°C/min.

In vitro PTX release

In vitro PTX release was determined by a dialysis method. Briefly, 2.0 mg of lyophilized PTX-loaded nanoparticles were dispersed in 5.0 mL release medium [phosphate buffer solution (PBS) and 0.1% Tween 80] of pH 7.4 to form a suspension. The suspension was then placed in a cellulose dialysis membrane (dialysis tubes MW cutoff 12 kDa; Sigma). Then, the closed bag was immersed in a beaker containing 50.0 mL of PBS and 0.1% Tween 80 as the release medium. The beaker was placed in an orbital water bath shaking at 110 rpm at 37°C. At given time intervals, 1.0-mL aliquots were removed for analysis and replaced with the same volume of fresh release medium at the same temperature. Based on the standard curve, the samples were assayed for drug content. Cumulative drug release was calculated according to the results of triplicate measurements.

Mucoadhesion studies

Mucoadhesion studies of Cht and Cht-GSH nanoparticles were performed by mucus glycoprotein assay. Periodic acid/Schiff colorimetric method was used for determining the amount of free mucin to estimate the amount of adsorbed mucins on the nanoparticles. Schiff reagent was prepared by

adding 1.0 g basic fuchsin (Merck) to 100.0 mL water. Before use, 0.1 g sodium metabisulfite was added to each 6.0 mL of Schiff reagent, and the final solution was incubated at 37°C until it became pale yellow. Periodic acid reagent was prepared fresh by adding 10 μL of 50% (vol/vol) periodic acid solution to 7.0 mL of 7% (vol/vol) acetic acid solution.

Standard solutions of mucin (0.25, 0.5, 0.75, and 1.0 mg per 2.0 mL) were used to prepare standard calibration curves. After adding 0.20 mL periodic acid reagent to the samples, the samples were incubated at 37°C in a water bath for 2 hours. Then, at room temperature, 0.20 mL Schiff reagent was added to the samples. After 30 minutes the absorbance of the solution was recorded at 555 nm in an ultraviolet spectrophotometer. Samples were run twice. For determining the mucoadhesion of the nanoparticles, a mucin solution (0.5 mg/mL) was prepared. Ten milligrams of the nanoparticles were vortexed in 6 mL of the mucin solution and shaken for 1 hour at 37°C. The suspensions were then ultracentrifuged for 5 minutes at 12,000 rpm, and the supernatant was analyzed for the free amount of mucin. The rest of the procedure was the same as for the standard solutions. Ethyl cellulose was used as negative control, and Carbomer 940 (Merck) was used as positive control for comparison purposes. Also, both controls were assessed with the same procedure. A standard calibration curve was used for calculating the mucin content in nanoparticles.[18,19]

Cytotoxicity assay

Cytotoxicity was assessed using MTT to assess the viability of the cells.[20] Cells from different cell lines were seeded in 96-well plates at the density of 8000–10,000 viable cells per well and incubated for 48 hours to allow cell attachment. The cells were then incubated for another 48 hours with nanoparticles without drug (Cht, Cht-GSH) and PTX-loaded nanoparticles (Cht–3% PTX, Cht–GSH–3% PTX). Cells were then washed in PBS, and 20 μL of MTT solution (5 mg/mL) were added to each well. The plates were incubated for an additional 4 hours, and then the medium was discarded. Dimethyl sulfoxide (60 μL) was added to each well, and the solution was vigorously mixed to dissolve tetrazolium dye. The absorbance of each well was measured by enzyme-linked immunosorbent assay reader (Anthous 2020; Anthos Labtec Instruments, Salzburg, Austria) at a test wavelength of 570 nm against a standard reference solution at 690 nm.

Statistical data analysis

Results are shown as mean ± SD. Statistical data analyses were performed using statistical software program (SPSS 15; Microsoft, Chicago, Illinois). The data were compared using the Student's *t*-test with $P < 0.05$ as the minimal level of significance.

Results

Chitosan depolymerization and characterization

Low molecular weights of Cht were necessary for achieving core-shell nanoparticles in the desired size range; hence, an oxidative degradation of Cht was applied.

Table 3
Encapsulation efficiency and drug loading of PTX-loaded Cht_{low}-GSH nanoparticles (n = 3)*

PTX-loaded nanoparticles (%)	Drug added (mg)	Encapsulation efficiency (%)	Drug loading (%)
Cht_{low}–GSH–1% PTX	2.7	95.31 ± 5.32	5.76 ± 0.68
Cht_{low}–GSH–2% PTX	5.4	95.17 ± 5.73	8.42 ± 2.30
Cht_{low}–GSH–3% PTX	8.1	98.27 ± 1.11	12.04 ± 3.71
Cht_{low}–GSH–4% PTX	10.9	97.67 ± 2.12	14.56 ± 1.12
Cht_{low}–GSH–5% PTX	13.6	97.83 ± 2.80	24.51 ± 4.45

Cht, chitosan; GSH, L-Glutathione reduced form; PTX, paclitaxel.

* For the thiolated Cht nanoparticles the standard errors for low, medium, and high molecular weight are 5.73, 4.41, and 3.96, respectively. For the nonthiolated Cht nanoparticles the standard errors for low, medium, and high molecular weight are 5.98, 5.69, and 8.81, respectively. The standard errors for ethyl cellulose and Carbomer 940 (Merck) are 3.84 and 6.23, respectively.

Molecular weights of hydrolyzed chitosans were determined by GPC using pullulane standards (Showa Denko, Kawasaki, Japan). The results are shown in Table 1. It can be seen that the molecular weights are in accordance with expected theoretical values and that increasing the amount of $NaNO_2$ reduced the molecular weight of the depolymerized Cht.

Thiolated chitosan preparation and quantification

The numbers of free-thiol groups, disulfide bonds, and total sulfhydryl groups immobilized on Cht-GSH were determined using iodine titration, and the results are shown in Table 1. Our results for thiol content of different molecular weights of Cht are in agreement with those reported before.[21] The maximum and minimum amount of free-thiol groups, disulfide bonds, and total amount of sulfhydryl groups were measured for Cht_{low} (92.81, 594.51, and 687.32 μmol/g) and Cht_{high} (75.77, 491.31, 567.08 μmol/g), respectively (Table 1).

Characterization of nanoparticles

Mean hydrodynamic diameter, polydispersity index (PDI), and zeta potential of blank and PTX-loaded nanoparticles prepared with different molecular weights of Cht and Cht-GSH are shown in Table 2. Nanoparticles showed a narrow size distribution (PDI < 0.443), positive zeta potential, and a size range of about 130–250 nm.

Surface morphology of nanoparticles

Nanoparticles of pMMA coated by Cht-GSH prepared in this study were spherical without aggregation. SEM images of nanoparticles are shown in Figure 1. Figure 2 shows a TEM image of the nanoparticles.

Drug encapsulation efficiency and drug loading

The loading characteristics of PTX nanoparticles are presented in Table 3. PTX was incorporated into the nanoparticles simultaneously during the preparation process of nanoparticles. The maximum encapsulation efficiency was 98.27%, and the maximum drug loading was 24.51%.

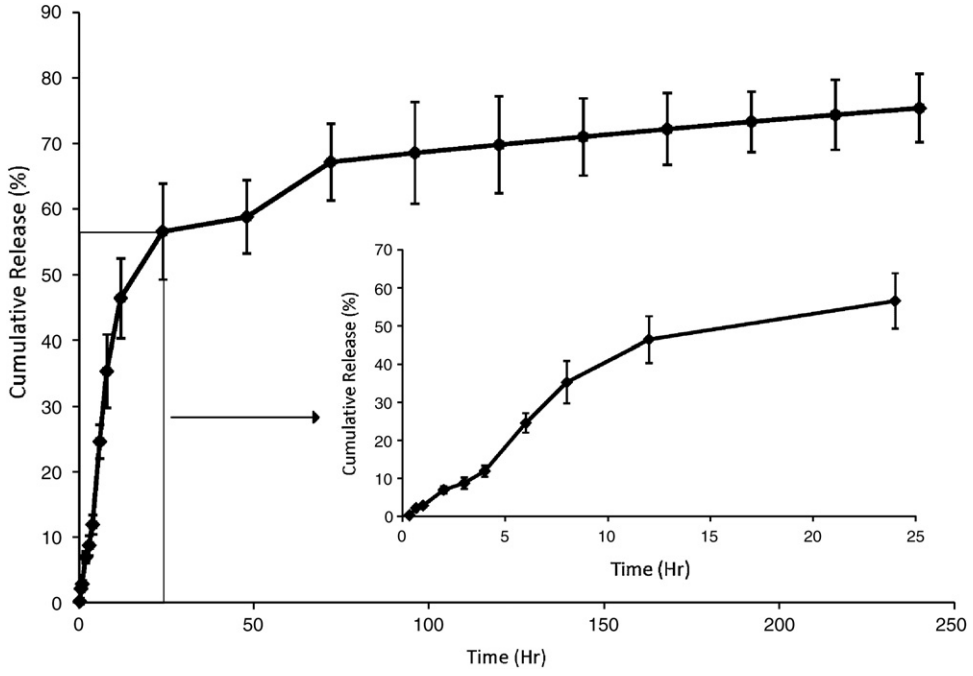

Figure 3. In vitro release of paclitaxel from paclitaxel-loaded poly(methyl methacrylate) nanoparticles coated with Cht-GSH-coated in phosphate buffer solution (pH 7.4) containing 0.1% Tween 80 at 37°C (n = 3).

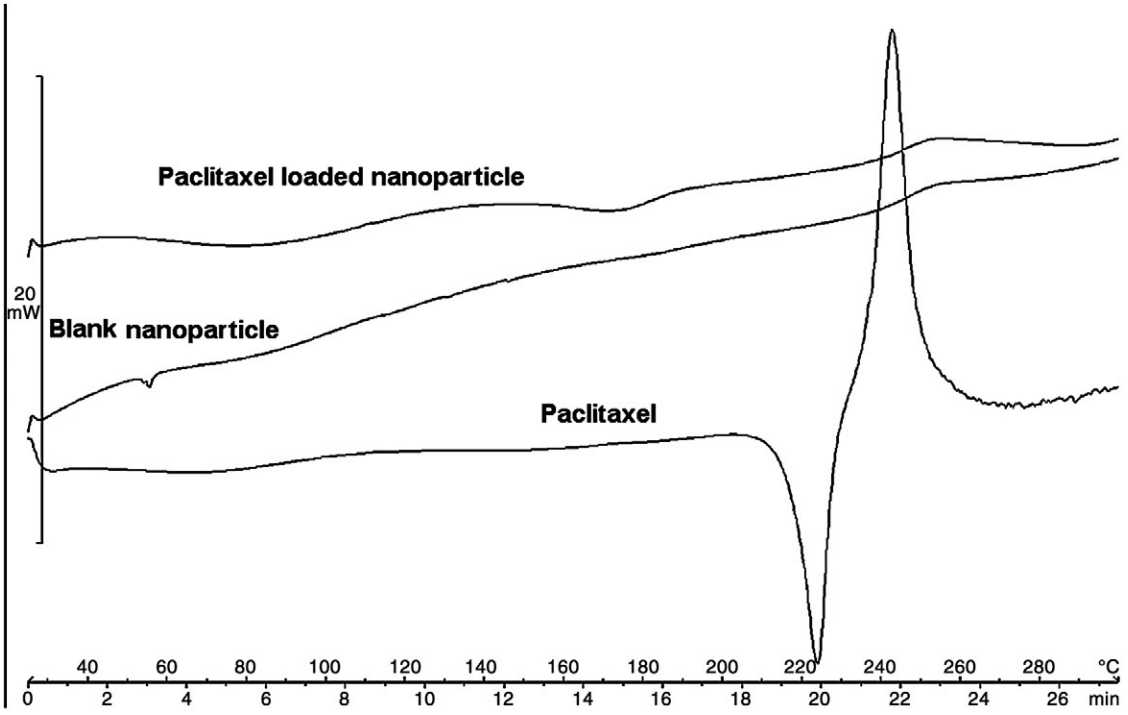

Figure 4. Differential scanning calorimetry thermograms of the pure paclitaxel (PTX), blank nanoparticles, and PTX-loaded nanoparticles.

In vitro drug release studies

To evaluate the potential of pMMA nanoparticles coated with Cht-GSH as a drug carrier for PTX, the in vitro release profile of PTX-loaded nanoparticles was investigated in PBS (pH 7.4) containing 0.1% Tween 80 at 37°C. The cumulative percentage release of Cht_{low}–GSH–3% PTX (14.67% drug loading) is shown in Figure 3. As can be seen, after 24 hours 56% of PTX had been released, followed by a sustained release of 75% until 240 hours.

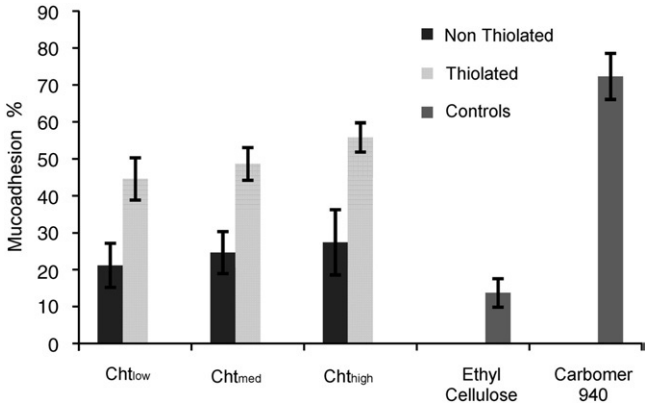

Figure 5. Mucoadhesion (%) of nanoparticles containing different molecular weights of non-thiolated chitosan (Cht) and Cht–L-glutathione reduced form (Cht-GSH, thiolated) in comparison with controls (n = 3).

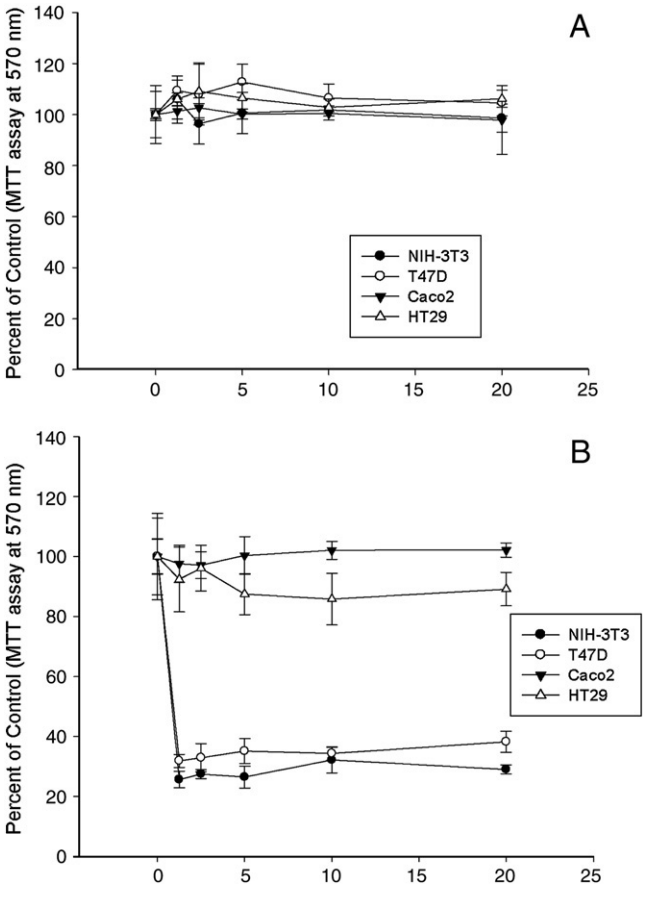

Figure 6. The effect of nonthiolated nanoparticles on the viability of cell lines (mean ± SD). **(A)** Chitosan; **(B)** chitosan–3% paclitaxel.

Physical status of paclitaxel in the nanoparticles

Physical status of PTX in the nanoparticles was examined by DSC (Figure 4). The melting endothermic peak of pure PTX appeared at 225°C. However, for the drug-loaded nanoparticles, no melting peak could be detected.

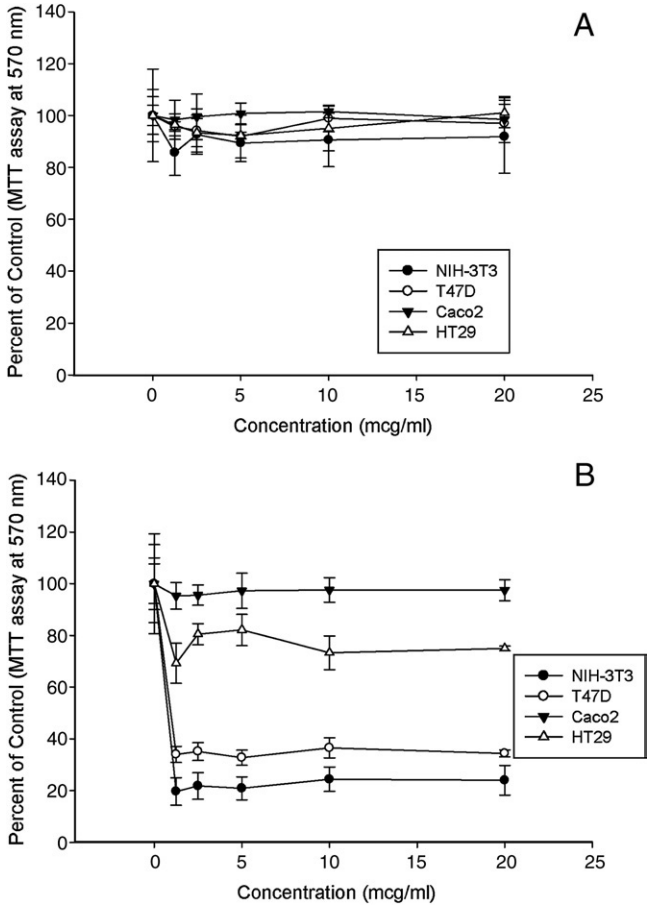

Figure 7. The effect of thiolated nanoparticles on the viability of cell lines (mean ± SD). **(A)** chitosan–L-glutathione reduced form (Cht-GSH); **(B)** Cht-GSH-3% paclitaxel.

Mucoadhesion study

The mucoadhesion percentages of Cht and Cht-GSH with different molecular weights are shown in Figure 5. The mucoadhesive behavior of Cht nanoparticles was estimated by suspending Cht nanoparticles in mucin aqueous solutions at room temperature. As can be seen in Figure 5, Cht-GSH nanoparticles with different molecular weights showed higher mucoadhesion in comparison with Cht nanoparticles. Also, both Cht and Cht-GSH nanoparticles with different molecular weights had more mucoadhesion than the negative control.

Cytotoxicity assay

MTT tests showed that PTX-loaded nanoparticles had different toxicity for different cell lines as can be seen in Figures 6 and 7. The Cht–3% PTX and Cht–GSH–3% PTX nanoparticles were very toxic for NIH 3T3 and T47D breast carcinoma cells, but they showed no toxicity for two colon cell lines (HT29, Caco2). Also, none of the blank Cht and Cht-GSH nanoparticles were toxic for the different cell lines applied in this study (Figures 6 and 7). As was shown, thiolating Cht did not increase its cytotoxicity.

Discussion

To form core-shell nanoparticles by radical polymerization of MMA, low molecular weights of Cht were essential.[22] Thus, depolymerization of medium-molecular-weight Cht (400 kDa) to different molecular weights was carried out via oxidative degradation by changing the amount of $NaNO_2$, in which an increase in the amount of $NaNO_2$ leads to lower molecular weights.[23]

Conjugates with higher molecular weights of Cht contain fewer free-thiol groups and disulfide bonds (Table 1)—possibly because the free amino groups of higher molecular weight Cht are not as accessible by the GSH molecule.

The formation of disulfide bonds between the thiomers and glycoproteins of mucus, which have cysteine-rich subdomains, is the basis of the main mechanism of thiomers mucoadhesion. The activity of the thiol groups of the conjugate has the fundamental role in the exchange reaction. GSH is a tripeptide with high conformational flexibility and is susceptible to oxidation and disulfide bond formation.[24] All thiolated chitosans revealed a higher amount of total sulfhydryl groups in comparison with free-thiol groups. It can be shown that the formation of intra- and/or intermolecular disulfide bonds is possible. This was also suggested for other thiolated products.[25] GSH can fix on amino groups that are far enough from each other in Cht_{high} to prevent disulfide bond formation. Also, that Cht_{high} contains fewer free-thiol groups means that fewer disulfide bonds will form. In Cht_{low}, GSH is immobilized on positions closer to amino groups, and its mobility and polymer short chains lead to the formation of intra- and/or intermolecular disulfide bonds. In addition, Cht_{low} contains a greater number of sulfhydryl groups. Thus, the formation of disulfide bonds and creation of cross-linked structure is greater. It should be mentioned that the presence of a cross-linked structure is not a disadvantage in the development of drug delivery systems, and they are useful in the control of the drug release.[21]

The nanoparticles were prepared based on a radical polymerization method. Cerium ions initiated the reaction and produced Cht or Cht-GSH radicals, which were ready to start the polymerization when MMA monomers were added to the medium. This reaction led to the formation of Cht-pMMA or Cht-GSH-pMMA copolymers, which were able to automatically form the nanoparticles.[17]

One of the most important parameters in determining the cellular uptake of the nanoparticles is the particle size. Increasing the particle size of the nanoparticles from approximately 500 nm decreases the permeability of the particles through the intestinal mucosa.[26] As can be seen in Table 2, the diameter of the nanoparticles prepared in this project ranged between about 130 nm and 250 nm—in the size range favoring the intestinal uptake of the nanoparticles.[27] Thiolated and nonthiolated nanoparticles did not differ significantly in size ($P < 0.6$). However, increasing the molecular weight of Cht increased the size of the nanoparticles, and vice versa ($P < 0.001$). Also, incorporating PTX in the nanoparticles did not affect the size of the nanoparticles ($P < 0.659$). Table 2 presents that all nanoparticles carried positive charge. Positive value of zeta potential is obviously due to the presence of Cht at the surface of the nanoparticles. In blank nanoparticles, Cht-GSH nanoparticles showed more zeta potential than Cht nanoparticles ($P < 0.05$). Although in Cht-GSH some amine groups are bound to GSH, and lower zeta potentials are thus expected, the free amino groups of GSH countered this effect and all Cht-GSH nanoparticles showed higher positive zeta potential than Cht nanoparticles. The presence of GSH on the surface of the PTX-loaded nanoparticles and incorporation of the drug into the nanoparticles did not affect the zeta potential.

As can be observed in TEM images of nanoparticles (Figure 2), two separate layers can be seen, and thus, presumably the clear layer that surrounds the compact core represents Cht-GSH.

It can be observed in Table 3 that the encapsulation efficiencies of all nanoparticles were higher than 95.17%, which showed that nanoparticles could be an effective carrier for PTX. The loading and encapsulation efficiency of PTX into nanoparticles was determined by changing the amount of PTX incorporated into the nanoparticles. Our results suggest that increasing the amount of PTX does not have a significant effect on encapsulation efficiency ($P < 0.839$). However, it can be seen in Table 3 that the nanoparticles containing 3% (PTX/polymer wt/wt) achieved higher encapsulation efficiency. A possible explanation could be that when the ratio was less than 3% there was not a sufficient amount of PTX and when the ratio was more than 3% the excess amount of PTX crystallized and thus was not incorporated into the hydrophobic core. Our results indicated that drug loading increased from 5.76% to 24.51%, while the amount of PTX increased from 1% to 5% (wt/wt). Increasing the amount of PTX increases drug loading significantly ($P < 0.008$).

In vitro release studies for the PTX-loaded nanoparticles show a relatively fast release of PTX in the first 48 hours, followed by a sustained release up to 240 hours. The fast release of PTX in the first 48 hours might be attributed to the diffusion and dissolution of PTX that was not efficiently entrapped in the polymer matrix. On the other hand, because there is a strong affinity between PTX and the hydrophobic core of the nanoparticles, the slower and sustained release might be due to the diffusion of PTX localized in the pMMA core. Also, the cross-linked structure of the Cht-GSH in the shell of the nanoparticles controlled the release rate of PTX from the nanoparticles. Our results suggest that the system of pMMA nanoparticles coated with Cht-GSH has the potential for sustained drug delivery and suppression of the adverse reactions related to PTX. Similar results have been reported.[6,28]

It can be seen from DSC thermograms (Figure 4) that no melting peak for PTX was detected in PTX-loaded nanoparticles. Thus, PTX in the nanoparticles was in a disordered crystalline phase or an amorphous or a solid-solution state.[26]

Because there is a strong interaction between Cht and mucin, mucin is adsorbed to the surface of Cht nanoparticles. Thus, a mucus glycoprotein assay was performed. Ethyl cellulose was used as a negative control and Carbomer 940 (Merck) as a positive control. Both controls were also assessed with the same procedure. After 1 hour of incubation, the free-mucin concentration was determined. Before and after adsorption of mucin on Cht nanoparticles, the amount of mucin adsorbed was determined from the free-mucin concentration in the reaction. The results suggest that the adsorption of mucin on Cht-GSH nanoparticles is greater than that on Cht nanoparticles ($P < 0.003$) (Figure 5). Increasing the molecular weight in both Cht-GSH and Cht nanoparticles increases mucoadhesion. However, this increase is not significant.

That no noticeable cytotoxicity of Cht and Cht-GSH nanoparticles was found in the MTT assay (Figures 6 and 7) indicates that the nanoparticles had satisfactory biocompatibility. However, there was a clear correlation found between cytotoxicity (MTT) for NIH 3T3 and T47D cells, and the presence of PTX in the nanoparticles (Figures 6 and 7). IC_{50} value of 3T3 cells in this study is found to be 1.5.[29] This result indicates that the nanoparticles were able to transport more PTX into the cells, thus achieving greater cytotoxicity with less PTX. Despite the evident cytotoxicity observed in T47D cells, the IC_{50} values were higher than earlier reported values.[30] Cht–3% PTX and Cht–GSH–3% PTX nanoparticles revealed no conspicuous cytotoxicity for HT29 and Caco2 cell lines, indicating that the nanoparticles could not enter the cells as a result of size constraints.

In conclusion, pMMA nanoparticles coated with Cht and Cht-GSH were prepared by radical polymerization. The nanoparticles were developed for administration of poorly soluble anticancer drugs, with PTX used as a model drug. The nanoparticles obtained were generally monodispersed spheres. The particle size was influenced by molecular weight. The surface charges of all nanoparticles were positive. High encapsulation efficiency of PTX was achieved, and the maximal encapsulation efficiency was up to 98.27%. In vitro studies demonstrated a sustained release of PTX for up to 10 days. The presence of either Cht or Cht-GSH on the surface of the nanoparticles clearly improved the mucoadhesion behavior of the nanoparticles. The PTX-loaded nanoparticles showed obvious cytotoxicity for NIH 3T3 and T47D breast carcinoma cells and no toxicity for two colon cell lines (HT29, Caco2). Introducing GSH on the surface of Cht nanoparticles did not increase its cytotoxicity. Briefly, the nanoparticles prepared in this study may represent a new delivery vehicle for hydrophobic anticancer drugs such as PTX.

References

1. Spencer CM, Faulds D. Paclitaxel. A review of its pharmacodynamic and pharmacokinetic properties and therapeutic potential in the treatment of cancer. Drugs 1994;48:794-847.
2. Rowinsky EK, Donehower RC. Paclitaxel (Taxol). N Engl J Med 1995; 333:75-81.
3. Schiff P, Fant J, Horwitz SB. Promotion of microtubule assembly in vitro by Taxol. Nature 1979;277:665-7.
4. Koziaraa JM, Lockmanb PR, Allenb DD, Mumper RJ. Paclitaxel nanoparticles for the potential treatment of brain tumors. J Control Release 2004;99:259-69.
5. Tarr BD, Yalkowsky SH. A new parenteral vehicle for the administration of some poorly soluble anti-cancer drugs. Parenter Sci Technol 1987;41: 31-3.
6. Danhier F, Lecouturier N, Vroman B, Jerome C, Marchand-Brynaert J, Feron O, et al. Paclitaxel-loaded PEGylated PLGA-based nanoparticles: in vitro and in vivo evaluation. J Control Release 2009;133:11-7.
7. Singla K, Garg A, Aggarwal D. Paclitaxel and its formulations. Int J Pharm 2002;235:179-92.
8. Leroux JC, Doelker E, Gurny R. The use o obtained f drug-loaded nanoparticles in cancer chemotherapy. In: Benita S, editor. Microencapsulation. New York: Marcel Dekker; 1996. p. 535-75.
9. Thanou M, Verhoef J, Junginger H. Oral drug absorption enhancement by chitosan and its derivatives. Adv Drug Deliv Rev 2001;52: 117-26.
10. Aghaei Moghaddam F, Atyabi F, Dinarvand R. Preparation and in vitro evaluation of mucoadhesion and permeation enhancement of thiolated chitosan-pHEMA core-shell nanoparticles. Nanomedicine 2009;5:208-15.
11. Lemarchand C, Gref R, Couvreur P. Polysaccharide-decorated nanoparticles. Eur J Pharm Biopharm 2004;58:327-41.
12. Bernkop-Schnurch A, Kast CE. Chemically modified chitosans as enzyme inhibitors. Adv Drug Deliv Rev 2001;52:127-37.
13. Bernkop-Schnurch A. Thiomers: a new generation of mucoadhesive polymers. Adv Drug Deliv Rev 2005;57:1569-82.
14. Atyabi F, Talaie F, Dinarvand R. Thiolated chitosan nanoparticles as an oral delivery system for Amikacin: in vitro and ex vivo evaluations. J Nanosci Nanotechnol 2009;9:4593-603.
15. Bernkop-Schnurch A, Kast CE, Guggi D. Permeation enhancing polymers in oral delivery of hydrophilic macromolecules: thiomer/GSH systems. J Control Release 2003;93:95-103.
16. Atyabi F, Aghaie Moghaddam F, Dinarvand R, Zohuriaan-Mehr MJ, Ponchel G. Thiolated chitosan coated poly hydroxyethyl methacrylate nanoparticles: synthesis and characterization. Carbohydr Polym 2008; 74:59-67.
17. Chauvierre C, Labarre D, Couvreur P, Vauthier C. Radical polymerisation of alkylcyanoacrylates initiated by the redox system dextran–cerium (IV) under acidic aqueous conditions. Macromolecules 2003;36: 6018-27.
18. Atyabi F, Majzoob S, Dorkoosh F, Sayyah M, Ponchel G. The impact of trimethyl chitosan on in vitro mucoadhesive properties of pectinate beads along different sections of gastrointestinal tract. Drug Dev Ind Pharm 2007;33:291-300.
19. He P, Davis SS, Illum L. In vitro evaluation of the mucoadhesive properties of chitosan microspheres. Int J Pharm 1998;166:68-75.
20. Mosmann T. Rapid colorimetric assay for cellular growth and survival: application to proliferation and cytotoxicity assays. J Immunol Methods 1983;65:55-63.
21. Bravo-Osuna I, Vauthier C, Farabollini A, Palmieri GF, Ponchel G. Mucoadhesion mechanism of chitosan and thiolated chitosan-poly (isobutyl cyanoacrylate) core-shell nanoparticles. Biomaterials 2007; 28:2233-43.
22. Bravo-Osuna I, Schmitz T, Bernkop-Schnurch A, Vauthier CF, Ponchel G. Elaboration and characterization of thiolated chitosan-coated acrylic nanoparticles. Int J Pharm 2006;316:170-5.
23. Huang M, Khor E, Lim LY. Uptake and cytotoxicity of chitosan molecules and nanoparticles: effects of molecular weight and degree of deacetylation. Pharm Res 2004;21:344-56.
24. Kafedjiiski K, Foge F, Werle M, Bernkop-Schnurch A. Synthesis and in vitro evaluation of a novel chitosan–glutathione conjugate. Pharm Res 2005;22:1480-8.
25. Bilicic MB, Filipovic-Grcic J, Martinac A, Barbaric M, Zorc B, Cetina-Cizmek B, et al. Synthesis and characterization of thiomers of polyaspartamide type. Int J Pharm 2005;291:211-9.
26. Feng SS, Mei L, Anitha P, Gan CW, Zhou W. Poly(lactide)–vitamin E derivative/montmorillonite nanoparticle formulations for the oral delivery of Docetaxel. Biomaterials 2009;30:3297-306.
27. Win KY, Feng SS. Effects of particle size and surface coating on cellular uptake of polyeric nanoparticles for oral delivery of anticancer drugs. Biomaterials 2005;26:2713-22.
28. He M, Zhao Z, Yin L, Tang C, Yin C. Hyaluronic acid cotaed poly(butyl cyanoacrylate) nanoparticles as anticancer drug carriers. Int J Pharm 2009;373:165-73.
29. Pauillard V, Nicolaou A, Double JA, Philips RM. Methionine dependence of tumours : a biochemical strategy for optimizing paclitaxel chemosensitivity in vitro. Biochem Pharmacol 2006;71: 772-8.
30. Bakogeorgoua E, Hatzogloub A, Castanasc E. Taxol inhibits opioid binding on T47D human breast cancer cells. Biochem Biophys Res Commun 1997;235:201-4.